Published in final edited form as:

J Immunol. 2017 November 01; 199(9): 3074–3085. doi:10.4049/jimmunol.1601880.

In Utero Exposure to Histological Chorioamnionitis Primes the Exo-Metabolomic Profile of Preterm CD4+ T Lymphocytes[1]

Poojitha Matta[*], **Stacy D. Sherrod**[†], **Christina C. Marasco**[‡], **Daniel J. Moore**[*], **John A. McLean**[†], and **Joern-Hendrik Weitkamp**[*]

[*]Department of Pediatrics, Vanderbilt University Medical Center and Monroe Carell Jr. Children's Hospital at Vanderbilt, Nashville, Tennessee, USA

[†]Department of Chemistry, Vanderbilt University, Nashville, Tennessee, USA

[‡]Department of Physics, Vanderbilt University, Nashville, Tennessee, USA

Abstract

Histological chorioamnionitis (HCA) is an intrauterine inflammatory condition increasing the risk for preterm birth, death, and disability due to persistent systemic and localized inflammation. The immunologic mechanisms sustaining this response in the preterm newborn remain unclear. We sought to determine the consequences of HCA exposure on the fetal $CD4^+$ T lymphocyte exo-metabolome. We cultured naïve $CD4^+$ T lymphocytes from HCA-positive and HCA-negative preterm infants matched for gestational age, sex, race, prenatal steroid exposure, and delivery mode. We collected conditioned media samples before and after a 6 hour *in vitro* activation of naïve $CD4^+$ T lymphocytes with soluble *Staphylococcal enterotoxin B* (SEB) and anti-CD28. We analyzed samples by ultra performance liquid chromatography ion mobility-mass spectrometry (UPLC-IM-MS). We determined the impact of HCA on the $CD4^+$ T lymphocyte exo-metabolome and identified potential biomarker metabolites by multivariate statistical analyses. We discovered that: (1) $CD4^+$ T lymphocytes exposed to HCA exhibit divergent exo-metabolomic profiles in both naïve and activated states; (2) ~30% of detected metabolites differentially expressed in response to activation were unique to HCA-positive $CD4^+$ T lymphocytes; and (3) metabolic pathways associated with glutathione detoxification and tryptophan degradation were altered in HCA-positive $CD4^+$ T lymphocytes; and (4) flow cytometry and cytokine analyses suggested a bias towards a T_H1-biased immune response in HCA-positive samples. HCA exposure primes the neonatal adaptive immune processes by inducing changes to the exo-metabolomic profiles of fetal $CD4^+$ T lymphocytes. These exo-metabolomic changes may link HCA exposure to T_H1 polarization of the neonatal adaptive immune response.

[1]This work was funded in part by the Eunice Kennedy Shriver National Institute of Child Health and Human Development (HD061607 to J.-H.W.) and the National Heart, Lung, and Blood Institutes (NIH, U01 HL101456 to J. L. A.), the National Institutes of Health's National Center for Advancing Translational Sciences (5UH3TR000491-04 to S.D.S.) as well as from funds from the Department of Pediatrics, Vanderbilt University Medical Center. The REDCap database was utilized for data collection and analysis through CTSA award No. UL1 TR000445 from the National Center for Advancing Translational Sciences (NIH).

Corresponding Author Information. Joern-Hendrik Weitkamp, MD, FAAP, Phone: (615) 322-3476, Fax: (615) 343-6182, hendrik.weitkamp@vanderbilt.edu.

Keywords

Human; Premature Birth; Chorioamnionitis; T cells; Cell Differentiation; Metabolome

INTRODUCTION

Preterm birth remains the leading cause of neonatal morbidity and mortality in the United States[1] and across the globe[2]. The most common causes include spontaneous preterm labor and premature rupture of membranes[3]. Both share a close association with histological chorioamnionitis (HCA)[4–6], an inflammation of the fetal membranes typically caused by intrauterine bacterial infection[7]. Fetal exposure to HCA induces *in utero* immune activation, resulting in fetal inflammatory response syndrome (FIRS), and shapes the neonatal transcriptomic immune response[8–10]. Clinical characteristics of FIRS consist of systemic inflammation and elevation of fetal plasma interleukin (IL)-6 and other pro-inflammatory cytokine levels[11]. Long-term sequelae of the sustained systemic inflammation precipitated by fetal exposure to HCA include blindness[12], cerebral palsy[13], impaired cardiac function[14], lung disease[15], and disruption of normal fetal immune development[16–20].

Recent studies on fetal sheep have demonstrated activation of the adaptive immune system following exposure to HCA[21]. Furthermore, umbilical cord blood derived from human neonates with clinical evidence of perinatal infection exhibited a higher proportion of Type 1 T helper (T_H1) cells than umbilical cord blood from uninfected neonates[22]. Activation and differentiation of $CD4^+$ T lymphocytes is thought to be tightly regulated by cellular metabolism[23]. However, data on metabolic changes induced by premature activation of fetal $CD4^+$ T lymphocytes remain limited. This deficit hinders the identification of therapeutic targets and further research on the severe and lifelong complications of premature birth following exposure to HCA.

Within the adaptive immune system, naive and activated $CD4^+$ T lymphocytes communicate through many different means, mediating their effects and thereby ensuring the production of an effective immune response. The secretion of metabolites constitutes one such critical mode of inter-cellular communication as molecular secretions often provide direction for and regulate collective cellular actions including naïve $CD4^+$ T lymphocyte activation and proliferation. Thus, the ability to study molecular secretions in the developing fetal adaptive immune system may provide insight into normal and atypical aspects of fetal adaptive immune processes resulting from fetal exposure to HCA.

We sought to assess changes in the exo-metabolomic profiles of fetal naïve $CD4^+$ T lymphocytes exposed to HCA following *in vitro* activation, using ion mobility-mass spectrometry, a highly specific analytical process that allows for small volume, complex biological samples to be analyzed with a high-throughput and unbiased approach. After comparing the exo-metabolomic profiles of fetal $CD4^+$ T lymphocytes isolated from matched HCA-positive and -negative infants, we putatively identified metabolites and candidate biochemical pathways that may function as biomarkers of HCA-induced reconditioning of fetal adaptive immune processes. These metabolic pathways may also

function as possible targets for the prevention of inflammatory sequelae resulting from *in utero* exposure to HCA.

MATERIALS AND METHODS

Experimental Design

Sample collection and study populations—This study was approved by the Vanderbilt University Medical Center (VUMC) Institutional Review Board (protocols #090161 and #110833). Peripheral blood mononuclear cells (PBMCs) were collected prospectively from premature infants admitted to VUMC neonatal intensive care unit on postnatal days 3, 7, 14, and 28. PBMCs were isolated and stored in liquid nitrogen. From this repository, we identified 10 individual samples of preterm patients exposed to HCA and 10 individual HCA-negative samples with similar gestational age, race, sex, and mode of delivery (Table I). All 20 mothers received prenatal steroids; most were exposed to prenatal antibiotics. All patients were exposed to postnatal antibiotics. Presence of funisitis in HCA-positive patients was determined upon review of the surgical pathology report. Two sample t-tests assuming unequal variances were conducted on each variable to determine statistical similarity/difference between the two sample groups.

Naïve $CD4^+$ T lymphocyte purification and activation—We isolated naïve $CD4^+$ T lymphocytes from PBMCs using an indirect magnetic labeling system (Miltenyi Biotec, Auburn, CA), as previously reported[24]. Briefly, $CD45RO^+$ and non-$CD4^+$ T lymphocytes were magnetically labeled using a biotin-conjugated antibody and anti-biotin microbead cocktail, according to manufacturer instructions. Isolation of naïve $CD4^+$ T lymphocytes is achieved by depletion of magnetically labeled cells with ≥ 90% purity.

Following sorting, the cell suspension was centrifuged to remove sorting buffer and re-suspended in RPMI medium supplemented with 10% Human AB Serum (Sigma, St. Louis, MO) and 1% Penicillin Streptomycin (Thermo-Fisher, Grand Island, NY). We cultured purified naïve $CD4^+$ T lymphocytes in 96-well microtiter plates, 40,000 cells $well^{-1}$. Immediately after plating, we collected 100 μL of conditioned media from all samples. Naïve $CD4^+$ T lymphocytes were subsequently activated using 30 μL soluble SEB (1 μg mL^{-1}, kindly provided by Michael J. Rosen, MD, MSCI, Cincinnati Children's Hospital Medical Center) and 30 μL anti-CD28 (10 μg mL^{-1}, BD Biosciences, San Jose, CA)[25]. Following 6 hours of incubation, at 37 °C, 100 μL of reconditioned media was collected from all samples and stored at −80 °C (Fig. S1a)[26].

Sample preparation for mass spectrometry—Samples were prepared for reverse phase (C_{18}) IM-MS and analyzed as previously reported[27] and shown in Fig. S1b. Briefly, we performed a cold methanol (Optima LC-MS grade, Fisher Scientific, Pittsburgh, PA) protein precipitation and dried the supernatants *in vacuo* (SpeedVac concentrator, Thermo-Fisher). Desiccates were reconstituted in 100 μL of 0.1% formic acid in water (LC-MS grade, Fisher Scientific). Quality control samples were prepared by combining equal volumes (15 μL) of each sample.

Mass spectrometry—UPLC-IM-MS and data-independent acquisition was performed on a Waters Synapt G2 (Milford, MA, USA) mass spectrometer equipped with a Waters nanoAcquity UPLC system and autosampler (Milford, MA, USA). Metabolites were separated on a 1 mm × 100 mm T3 column packed with 1.8-μm, 10-nm high strength silica (HSS) particles (Waters, Milford, MA, USA). Liquid chromatography was performed using a 25-minute gradient at a flow rate of 70 μL min^{-1} using solvent A (0.1% formic acid (FA) in H_2O) and solvent B (0.1% FA with acetonitrile). 99% of solvent A is initially perfused with a linear gradient applied such that solvent A is decreased to 1% and solvent B increased to 99% over 12 min. This condition is held for 3 min. The solvent percentage is then returned to the initial state in the next minute (99% solvent A, 1% solvent B) and held for 9 min to re-equilibrate the column.

Typical IM-MS analyses were run using resolution mode, with a capillary voltage of 3 kV, source temperature at 120 °C, sample cone at 35, desolvation temperature at 400 °C, He cell flow of 180 mL min^{-1}, and an IM gas flow of 90 mL min^{-1}. The data were acquired in positive ion mode from 50 to 2000 Da with a 0.5 s scan time; full-scan data were mass corrected during acquisition using an external reference consisting of 3 ng mL^{-1} solution of leucine enkephalin. All analytes were analyzed using MS^E with an energy ramp from 5 to 35 eV.

Analysis Strategy

Data processing—We converted acquired raw data to mzXML format using the Proteowizard msconvert tool (http://proteowizard.sourceforge.net/team.shtml)[28]. These files were then analyzed using XCMS in the R Studio statistical package, to peak pick and align features (i.e., retention time (RT) and mass-to-charge (m/z) ratio pairs). XCMS was used with default settings as described in http://metlin.scripps.edu/xcms/ except rector (method = “obiwarp”). Data were normalized to the summed total ion intensity per chromatogram, with the total ion count normalized to 10,000 counts.

Determination of exo-metabolomic differences—We analyzed the processed data matrix with multivariate statistical analysis using Umetrics extended statistics software EZInfo version 2.0.0.0 (Waters, Milford, MA). Orthogonal partial least squares-discriminant analysis (OPLS-DA) was performed on expression levels of all measurable analytes and used Pareto scaling to determine exo-metabolomic differences between HCA-positive and -negative samples in the naïve and activated states.

The integrated intensity of each chromatographically resolved m/z peak was $\log_2$ transformed. Change in peak area following $CD4^+$ T lymphocyte activation was determined using fold change (FC = mean ACTIVATED /mean NAIVE). Statistical significance was determined using a paired two-tailed Student’s *t*-test. Technical replicates were used in these calculations; all calculations were performed on $\log_2$ transformed values. An m/z species was considered differentially expressed when it met the dual criteria of fold change $|FC| > 1$ and *p*-value < 0.05 (for all subsequent analyses, *p*-value < 0.05 was used as the threshold for significance). Direction of change was defined as FC > 1 = produced, FC < −1 = consumed.

Additionally, for a differentially expressed metabolite to be changed due to HCA exposure, it had exhibit a magnitude difference (|FC| > 1) and *p*-value < 0.05 from control samples.

Identification of analytes by ion mobility – mass spectrometry—Volcano plot analyses were generated to compare exo-metabolomic differences between HCA-positive and -negative samples and determine metabolites of interest. The log2[FC] between HCA-positive and -negative samples was plotted along the x-axis and calculated using normalized abundance values. *P*-values were calculated using an unpaired two-tailed Student's *t*-test of equal variance to determine statistical significance of difference of group means values. Metabolites that showed a *p*-value < 0.05 were prioritized for identification. All analyses were performed on $\log_2$ transformed values.

Putative metabolite identifications were assigned using both mono-isotopic accurate mass measurements (<30 ppm) and fragmentation data (MS/MS analyses). Candidate structures were obtained and interpreted with available databases, including the Human Metabolome Database[29], METLIN[30], LIPID MAPS[31]. Additionally, acquired raw data were analyzed using Progenesis QI[32], a small molecule discovery analysis software for LC-MS data.

The statistical significance of putatively identified metabolites were analyzed between matched disease and control pairs. Significance was determined using two-way repeated measures (mixed-model) analysis of variance (ANOVA). Wilcoxon matched-pairs signed-rank tests were performed to determine the overall statistical significance between pairwise comparisons. All calculations were performed on ($\log_2$ transformed) normalized abundance values in Graphpad Prism.

Analysis of $CD4^+$ T lymphocyte cytokine production and phenotype

Flow cytometry—We analyzed phenotype, activation and cytokine profiles of $CD4^+$ T lymphocytes using multicolor flow cytometry. We stained viable cryopreserved PBMCs collected at post-natal days 3, 7, 14, and 28 using the following antibody panel: CD^3, CD^4, CD^8, CD^{45RO}, CD^{25}, CD^{69}, LFA-1, CD^{154} (CD^{40} ligand), CD^{127}, FOXP3, GARP, CCR4, CCR6, and CXCR3. An amine-reactive live-dead marker was used to exclude dead cells. A Becton Dickson LSR-II flow cytometer and FlowJo software (Tree Star) was used to analyze the data. Subsets of $CD4^+$ T lymphocytes were characterized using the following markers[33]: T_H1 ($CD45RO^+$ $CXCR3^+$ $CCR6^-$ $CCR4^-$). A comparable staining panel was used in a recent study to identify activated memory T_H1 and T_H2 lymphocytes in the cord blood of healthy term neonates[34].

Activation assay and analysis of cytokine production—Using the same repository as above, we identified 5 individual preterm infants exposed to HCA and 5 individual HCA-negative patients matched for gestational age, race, sex, mode of delivery, day of blood draw, and prenatal steroid exposure.

We isolated naïve $CD4^+$ T lymphocytes from PBMCs using an indirect magnetic labeling system (Miltenyi Biotec, Auburn, CA), as detailed above. We cultured purified naïve $CD4^+$ T lymphocytes in 96-well microtiter plates, 40,000 cells $well^{-1}$. Immediately after plating, we collected 100 μL of conditioned media from all samples. Naïve $CD4^+$ T lymphocytes

were subsequently activated using 10 ng mL^{-1} phorbol 12-myristate 13-acetate (PMA) (Sigma, St. Louis, MO) and 1 μg mL^{-1} ionomycin (Sigma, St. Louis, MO). Following 6 hours of incubation, at 37 °C, 100 μL of reconditioned media was collected from all samples. We confirmed > 95% cell viability at the end of the incubation period in our pilot experiments. Cytokines were subsequently measured using the Milliplex Map multiplex magnetic bead-based immunoassay kits (Millipore) on a Luminex Flexmap 3D Platform as reported previously[35]. A paired t-test was used to determine the statistical significance of differences in IFNγ secretion.

RESULTS

$CD4^+$ T lymphocytes of preterm infants exposed to HCA exhibited distinct exo-metabolomic signatures in both naïve and activated states

The mean gestational age at birth was nearly identical between both groups: HCA-positive: 27 weeks, HCA-negative: 26 weeks, 6 days (*p*-value: 0.69). The male to female ratio was identical both groups (*p*-value: 1); the HCA-positive group had 4 African-American samples and the HCA-negative group had 2, the remaining samples were Caucasian (*p*-value: 0.36). The HCA-positive group had equal proportions of cesarean and vaginal deliveries while the HCA-negative group had two vaginal deliveries and 8 cesareans (*p*-value: 0.18). The day of blood draw showed a statistically significant difference between the two groups (*p*-value: 0.04), while the differences in exposure to prenatal antibiotics were statistically insignificant (*p*-value: 0.15). All patients were exposed to postnatal antibiotics, particularly ampicillin and gentamicin, at least through day of life (DOL) 2. Notably, HCA-positive patients were exposed to antibiotics for a statistically longer period of time than HCA-negative patients (*p*-value: 0.03) (Table 1). All 20 mothers received prenatal steroids to promote fetal lung development. Histological signs of funisitis were found in 8 of 10 HCA-positive patients. Seven patients showed signs of Stage II FIRS and 1 patient showed signs of Stage I FIRS.

Following data processing (peak picking and alignment), we detected 1,652 unique exo-metabolomic features (each feature presents a unique combination of mass-to-charge ratio (m/z) and retention time (RT)). In order to study the metabolomic signatures of each sample type and differences between HCA-positive and –negative sample groups, we carried out a series of statistical analyses on all detected exo-metabolomic features.

We used OPLS-discriminant analysis to examine what, if any, differences exist between the exo-metabolomic signatures of HCA-positive and -negative samples. The OPLS-DA score plots in Fig. 1 display the exo-metabolomic signatures of each sample type. Fig. 1a shows the exo-metabolomic signature of naïve $CD4^+$ T lymphocytes, i.e. prior to SEB/CD28-induced activation, and Fig. 1b depicts the exo-metabolomic signature of activated $CD4^+$ T lymphocytes. Fig. 1a demonstrates a distinct separation between HCA-positive and -negative sample groups along OPLS1, resolving the two sample types into two discrete classes. This unambiguous between-group difference suggests sizable variations in the exo-metabolomic signatures of HCA-positive and -negative samples in the naïve state. Interestingly, the HCA-negative samples exhibit separation along OPLS2, suggesting a unique within-group variation not seen in the HCA-positive sample group. The two sample groups were similarly discretized along OPLS1 in the activated state (Fig. 1b), suggesting continued disparities in

the exo-metabolomic signatures of HCA-positive and -negative sample groups. The sizable within-group variation unique to the HCA-negative sample group persisted in the activated state.

We compared HCA-negative samples collected 5 days postnatal ($n = 4$) with samples collected 10 days postnatal ($n = 6$) for any potential bias. We determined that these HCA-negative samples behaved similarly, regardless of the date of sample collection. Therefore, the within-group variation exhibited by the HCA-negative sample group cannot be explained by the timing of sample collection.

The global exo-metabolomic profiles of both sample types were significantly altered in response to SEB/CD28 stimulation. To directly compare the production and consumption of metabolites in response to stimulation, significance criteria of $p < 0.05$ and $|FC| > 1$, were used. Of the original 1,652 species, 676 metabolites (41.0%) met the significance criteria for HCA-positive samples and 678 (40.9%) for HCA-negative samples.

HCA-positive and -negative samples demonstrated distinct responses to SEB/CD28-induced activation (Fig. 2a). Activation of HCA-negative cultures produced a total of 580 species (three upward arrows in HCA-negative circle in Fig. 2a) and consumed 98 (three downward arrows). 165 of the metabolites produced and 35 consumed were unique to the HCA-negative sample group, i.e. these 200 metabolites (29.5%) were not differentially expressed by HCA-positive samples. Likewise, activation of HCA-positive cultures produced a total of 584 metabolites (three upward arrows in HCA-positive circle in Fig. 2a) and consumed 92 (three downward arrows). 163 of the metabolites produced and 35 consumed, for a total of 198 metabolites (29.3%), were unique to the HCA-positive sample group.

As expected, the exo-metabolomic activity observed in HCA-positive samples showed a large overlap with exo-metabolomic activity seen in $CD4^+$ T lymphocytes derived from HCA-negative samples: of the 676 species produced or consumed by HCA-positive samples, 478 metabolites (70.7%) were common to both HCA-positive and –negative cultures, with 410 metabolites (60.7%) having the same directionality of change (consumed or produced). Overall, the responses of both sample groups to SEB/CD28 stimulation were dominated by exo-metabolome increases (i.e. production of metabolites).

Next, we used volcano plot analyses to directly compare the normalized abundance of individual metabolic species between HCA-positive and -negative sample types and highlight individual metabolites that met the significance criteria. Figure 2b shows two volcano plot analyses that compare all (1,652) detected metabolites in the naïve (left) and activated states (right). The log2[FC] is plotted along the x-axis (FC = mean $_{\text{HCA-POS}}$ /mean $_{\text{HCA-NEG}}$) and the statistical significance of this is shown along the y-axis (−log10 scale). Metabolites that display a positive log2[FC] are over-expressed (i.e. over produced) in HCA-positive samples while negative values indicate under-expression (i.e. over consumed) in the HCA-positive sample group. Statistically significant metabolic species ($p < 0.05$) are shown in blue while statistically insignificant species are represented in black. Identified metabolites are displayed in red and labeled.

Altogether, we detected 482 statistically significant species in naïve state. Of these, 411 (85.3%) metabolites showed a statistically significant positive log2[FC]; the remaining 71 (14.7%) species reflected statistically significant negative differences. Comparably, 442 statistically significant species were identified in the activated state. Of these, 376 (85.1 %) metabolic species showed a statistically significant positive log2[FC] while 66 (14.9%) exhibited negative differences, suggesting extensive changes in the production and consumption of metabolic species following exposure to HCA.

Identification of metabolic species with immune response modifier potential

Additionally, we used volcano plot analyses to produce a list of metabolic species (shown in blue, Fig. 2b) that were prioritized for identification. We putatively identified 5 metabolites: 4-Hydroxynonenal (4-HNE), 3-Hydroxykynurenine (3-HK), Dopamine (DA), Serotonin (5-HT), and LysoPC (18:2(9Z, 12Z)) (LPC) (Table II).

From the prioritized list of metabolic species, we putatively identified one metabolite 4-HNE (*m/z* 195.07, RT 1.03 min) that belongs to the glutathione (GSH) detoxification pathway (Fig. S3a). GSH levels have previously been shown to be important in determining the course of the adaptive immune response[36]. Analysis of 4-HNE in this mass spectrometry revealed relatively lower levels of 4-HNE in HCA-positive samples in the naïve state only (Fig. 3a, b). Statistical analyses using the Wilcoxon matched-pairs signed-rank test indicated a statistically significant difference in 4-HNE ($p < 0.05$) in naïve state only, suggesting that exposure to HCA may affect the 4-HNE detoxification process prior to the initiation of an adaptive immune response.

We also observed exo-metabolome changes in HCA-positive samples relating to the tryptophan metabolism pathway, which has previously shown to influence the development of the adaptive immune response[37]. Both putatively identified metabolites, 5-HT (*m/z* 177.08, RT 2.57 min) and 3-HK (*m/z* 225.09, RT 1.25), are downstream metabolites in the tryptophan pathway (Fig. S3b).

Overall, 5-HT was elevated in HCA-positive $CD4^+$ T lymphocytes in both naïve and activated states (Fig. 4a). Specifically, 9 of the 12 pairs showed greater normalized abundance of 5-HT in the HCA-positive sample in both naïve and activated states (Fig. S2a). Statistical analyses using the Wilcoxon matched-pairs signed-rank test indicate a significant difference in both naïve ($p < 0.01$) and activated ($p < 0.01$) states, suggesting that exposure to HCA may alter 5-HT metabolism before and after the initiation of an adaptive immune response.

The signal for 3-HK was also elevated in HCA-positive $CD4^+$ T lymphocytes in both naïve and activated states (Fig. 4b). Specifically, 5 of 12 matched pairs showed increased 3-HK signal in HCA-positive samples in both states (Fig. S2b). Statistical analyses using the Wilcoxon matched-pairs signed-rank test indicate a significant difference in both naïve ($p < 0.01$) and activated ($p < 0.05$) states, suggesting that exposure to HCA may modify 3-HK metabolism before and after the initiation of an adaptive immune response.

We have also putatively identified DA (*m/z* 176.07, RT 4.63 min), a metabolite in the catecholamine biosynthesis pathway (Fig. S3c) and LPC (18:2(9Z, 12Z)) (*m/z* 520.35, RT 10.49 min), which is formed through the hydrolysis of phosphatidylcholine by the phospholipase A2 (PLA2) (Fig. S3d). Statistical analyses using the Wilcoxon matched-pairs signed-rank test indicated no overall significant differences in DA (Fig. 5a, S2c) and LPC (18:2(9Z, 12Z)) (Fig. 5b, S2d) levels between HCA-positive and -negative samples in either state, suggesting that exposure to HCA does not impact DA and LPC (18:2(9Z, 12Z)) metabolism in the naïve and activated states.

Characterizing the phenotype of CD4$^+$ T lymphocytes and alterations in cytokine production following exposure to HCA

Lastly, we used fluorescence-based flow cytometry to interrogate differences in cell surface marker expression and identify any phenotypic features that may distinguish HCA-positive and HCA-negative CD4$^+$ T lymphocytes. We and others have shown that preterm infants exposed to HCA exhibit increased proportions of CD4$^+$ T lymphocytes expressing memory markers[73, 95]. We found decreases in the expression of CD4 and CD8 markers in the HCA-positive sample. Conversely, we found CD45RO, CXCR3, and CCR6 to be over-expressed in the HCA-positive sample (Fig. 6a). In addition, we used Luminex assays to determine changes in the cytokine production of activated CD4$^+$ T lymphocytes following exposure to HCA. We found significant increases in IFNγ production in HCA-positive samples (p-value = 0.0032) (Fig. 6b). Taken together, these data suggest a notable bias towards a T_H1 immune response in HCA-positive preterm infants.

DISCUSSION

Maintenance and regulation of CD4$^+$ T lymphocyte metabolic homeostasis is necessary for producing an effective immune response[38, 39]. Historically, fetal cytokine responses have been thought to be biased towards a Type 2 T helper (T_H2) phenotype to protect against fetal rejection[40]. On the other hand, increased fetal T_H1 cytokine production has been shown to increase the risk for inflammatory injury but has also been associated with improved immunity towards viral and fungal challenges[41]. Thus, a better understanding of mechanisms underlying the CD4$^+$ T lymphocyte exo-metabolome may help explain the seemingly contradictory outcomes of increased fetal T_H1 cytokine production and also point to novel therapeutic targets in the prevention of inflammatory injury following preterm birth and contribute towards the development of treatment options.

We have applied UPLC-IM-MS to produce the first exo-metabolomic profiles of naïve and activated CD4$^+$ T lymphocytes derived from human preterm infants with and without HCA exposure. While our approach has several limitations, we attempted to carefully match samples for known modulators of immune responses including exposure to prenatal steroids, delivery mode, sex, race and gestational age. We were not able to rule out other confounding variables, i.e. maternal smoking[42].

The availability of post-natal blood samples from extremely low birth weight infants combined with UPLC-IM-MS methodology did not allow us to test more than 20 individual patients. However, since we analyzed CD4$^+$ T lymphocyte exo-metabolomes prior to and

after activation, we were able to collect a large set of data from 40 separate samples. This allowed us to perform the appropriate statistical analyses. Lastly, our *in vitro* approach may not reflect the complexity of fetal immune activation associated with *in vivo* HCA exposure[43] but our approach provided a means for determining potentially important metabolites and associated pathways that could be critical to $CD4^+$ T lymphocyte metabolism and function in this vulnerable population, without *a priori* knowledge.

In utero exposure to HCA is known to prematurely activate the otherwise mostly dormant fetal adaptive immune response[44]; however, its postnatal effects on $CD4^+$ T lymphocyte function and metabolism have not yet been discerned. We discovered that exposure to HCA has a substantial and defined overall impact on $CD4^+$ T lymphocyte exo-metabolomic profiles in both naïve and activated states. This could indicate a positive correlation between fetal exposure to HCA and dysregulation of naïve $CD4^+$ T lymphocyte bioenergetics that is perpetuated in the activated state. An unexpected finding, however, was the sizable within-group variation exhibited by HCA-negative samples. This variation could be attributed to naturally occurring biological variability however, it is also possible that exposure to HCA induces a more uniform exo-metabolomic phenotype. While the timing of sample collection may explain this intra-group variation, we believe this to not be the case. Studying the postnatal dates of sample collection did not yield any clear patterns of association and although our sample size is limiting in this regard, we are confident that the date of sample collection did not contribute to this intra-group variation.

Both HCA-positive and -negative samples predominantly increased their metabolite production upon activation and the numeric extent of metabolite turnover was nearly identical between the two sample types. This large overlap in the levels of exo-metabolic activity is noteworthy, but expected considering that both sample groups are derived from the same cell type. However, despite similarities in the overall exo-metabolic activity, the production and consumption of specific metabolites in response to SEB/CD28-induced activation varied markedly between HCA-positive and -negative sample types: ~30% of metabolites produced/consumed were uniquely expressed by $CD4^+$ T lymphocytes derived from HCA-positive infants. This large divergence in the differential expression of specific metabolites supports a correlation between *in utero* HCA exposure and changes in the bioenergetics of naïve and activated $CD4^+$ T lymphocytes.

In follow-up analyses of the exo-metabolomic overlap we were able to discern additional distinctions in the differential expression levels of metabolites common to both sample types. Almost 60% of the metabolites differentially expressed by both sample groups were either over- or under-expressed by the HCA-positive sample group. These data indicate a connection between HCA exposure and metabolic dysregulation of fetal $CD4^+$ T lymphocytes.

We have putatively identified five distinct metabolites that, with further validation, could function as biomarkers of HCA exposure. These include 4-HNE, 5-HT, 3-HK, DA, and LPC. 4-HNE is widely known as an inducer of oxidative stress and a highly toxic end product of lipid peroxidation[45–47]. Thus, precise regulation of intracellular 4-HNE levels is necessary for cell survival. This molecule is largely depleted through GSH conjugation,

which is catalyzed by glutathione S-transferase[48, 49]. Consequently, the neutralization/detoxification process has been shown to be highly dependent on GSH levels[50]. Current evidence suggests that GSH is also of great importance to the initiation and progression of $CD4^+$ T lymphocyte activation[51–54]. Recent studies even point to a correlation between GSH deficiency and decreased levels of T_H1-associated cytokines (IL-2 & IFNγ)[55].

Our findings indicate decreased abundances of 4-HNE in HCA-positive $CD4^+$ T lymphocytes in the naïve state only. This discrepancy in 4-HNE levels may be due to increased GSH levels (and therefore increased rates of detoxification) in naïve HCA-positive samples. Although we are not certain as to why GSH levels would be selectively increased in the naïve state, this finding is consistent with existing data that suggest changes in GSH concentration can affect activation-dependent lymphocyte proliferation without regulating the activated functions of these cells[56].

In addition to altered 4-HNE metabolism, we observed changes in two metabolites that belong to the tryptophan metabolism pathway. As downstream metabolites of tryptophan, 5-HT and 3-HK abundances are directly indicative of tryptophan degradation patterns[57]. Existing data suggest a strong correlation between IFNγ production and sustained up-regulation of tryptophan degradation[58–61]. Posited as the *tryptophan depletion theory*, the details of this connection are not thoroughly understood; although, it is thought that IFNγ production precipitates this up-regulation[62]. IFNγ is a hallmark pro-inflammatory cytokine classically associated with the T_H1 adaptive immune response[63, 64]. In follow-up experiments, we have identified statistically significant increases in IFNγ production in activated $CD4^+$ T lymphocytes exposed to HCA, supporting our findings on changes to tryptophan degradation in HCA-positive $CD4^+$ T lymphocytes.

Our observations of increased 5-HT and 3-HK abundances in conjunction with amplified IFNγ production in HCA-positive samples suggests that exposure to HCA may be associated with the up-regulation of tryptophan degradation in naïve and activated $CD4^+$ T lymphocytes. Consequently, our data may indicate a correlation between HCA exposure and a T_H1 polarization of the fetal adaptive immune response.

We have also identified DA, a metabolite that belongs to the norepinephrine and epinephrine biosynthesis pathway. These two catecholamines have been shown to regulate lymphocyte function, *in vitro*[65, 66]. As the immediate precursor to NE and the preferential method for its synthesis, DA abundances are directly indicative of NE biosynthesis patterns[67]. Mouse studies have previously shown the production of catecholamines, including NE and EP, to have an important role in modulating T lymphocyte-mediated immune responses[68, 69]. In fact, elevated levels of these catecholamines in resting T lymphocytes have been shown to decrease production of IL-12 (a T_H1 promoting cytokine)[70]. Greater abundances of catecholamines in activated T lymphocytes are also known to impair the function of human effector T_H1 lymphocytes by suppressing IFNγ and IL-2 (pro-inflammatory cytokines) production and enhance the production of T_H2 (anti-inflammatory) cytokines[71–73]. Therefore, it was unsurprising for us to find comparable abundances of DA in naïve and activated HCA-positive and –negative samples. Our observations suggest that exposure to HCA does not impact DA metabolism in naïve or activated $CD4^+$ T lymphocytes. This may

be because HCA exposure induces a T_H1 polarization of the fetal adaptive immune response and normal catecholamine production is requisite for this type of immune response.

Lastly, we have also identified LPC (18:2(9Z, 12Z)), a bioactive pro-inflammatory lipid produced via the hydrolysis of plasma membrane phosphatidylcholine, a process catalyzed by the PLA2 enzyme[74]. Obstruction of this enzymatic function in animal models has been shown to diminish the development of T_H1 and T_H17 immune responses[75]. Mouse studies from the same research group have also shown cytosolic PLA2 deficient mice to be incapable of producing T_H1 type cytokines[76]. Considering our findings of comparable LPC abundances in naïve and activated HCA-positive and -negative samples, we believe HCA exposure does not impact LPC metabolism. This may be because *in utero* HCA exposure induces a T_H1 polarization of the fetal adaptive immune response, and consistent LPC metabolism is necessary for the initiation and production of this immune response.

A suitable balance between T_H1 and T_H2 adaptive immune responses that meets the immune challenge is necessary to avoid excessive inflammation/tissue damage (T_H1) and the over-promotion of allergic responses (T_H2)[77]. Preterm infants with evidence of perinatal infection exhibit a higher proportion of T_H1 cells than uninfected preterm infants[78], suggesting that exposure to HCA polarizes the fetal adaptive immune response towards the T_H1 type. Within the noted limitations of our study, our findings may indicate a possible mechanistic link between *in-utero* HCA exposure and T_H1 polarization of the fetal adaptive immune response. Validation studies will be necessary to confirm the immune biomarker role of the putatively identified metabolites in our study.

To summarize our results, we have shown for the first time that antenatal exposure to HCA induces changes in the bioenergetics of naïve and activated $CD4^+$ T lymphocytes of preterm infants, resulting in altered exo-metabolomic profiles. Putatively identified metabolites differentially secreted by HCA-positive $CD4^+$ T lymphocytes support existing literature, suggesting that exposure to HCA polarizes the adaptive immune response towards a T_H1 response. In addition to inflammatory injury associated with preterm birth, metabolic changes to the fetal immune processes resulting from *in utero* HCA exposure may explain the observed immune dysregulation we observed in this study, suggesting a critical role for the fetal environment in shaping normal and aberrant host responses of the developing infant.

Supplementary Material

Refer to Web version on PubMed Central for supplementary material.

Acknowledgments

The contents of this manuscript are solely the responsibility of its authors and do not necessarily represent the official views of funding agencies and/or organizations. Additionally, the relevant funding agencies and organizations had no role in the experimental design, collection, analysis, or interpretation of data, nor were they involved in the writing the manuscript and the decision to submit for publication. We appreciate the support of the SyBBURE-Searle Undergraduate Research Program, the Vanderbilt Institute for Integrative Biosystems Research and Education (VIIBRE), and the Vanderbilt Center for Innovative Technology (CIT). Additionally, we would like to acknowledge and thank Dr. John P. Wikswo of VIIBRE for his support and valuable comments.

References

1. Martin, JA. N. C. F. H. S. (US). Births: final data for 2003. US Department of Health and Human Services, Centers for Disease Control and Prevention, National Center for Health Statistics; 2005.
2. Beck S, Wojdyla D, Say L, Betran AP, Merialdi M, Requejo JH, Rubens C, Menon R, Van Look PF. The worldwide incidence of preterm birth: a systematic review of maternal mortality and morbidity. Bulletin of the World Health Organization. 2010; 88:31–38. [PubMed: 20428351]
3. Tucker JM, Goldenberg RL, Davis RO, Copper RL, Winkler CL, Hauth JC. Etiologies of preterm birth in an indigent population: is prevention a logical expectation? Obstetrics & Gynecology. 1991; 77:343–347. [PubMed: 1992395]
4. Hillier SL, Martius J, Krohn M, Kiviat N, Holmes KK, Eschenbach DA. A case-control study of chorioamnionic infection and histologic chorioamnionitis in prematurity. N Engl J Med. 1988; 319:972–978. [PubMed: 3262199]
5. Epstein FH, Goldenberg RL, Hauth JC, Andrews WW. Intrauterine infection and preterm delivery. New Engl J Med. 2000; 342:1500–1507. [PubMed: 10816189]
6. Steel JH, Malatos S, Kennea N, Edwards AD, Miles L, Duggan P, Reynolds PR, Feldman RG, Sullivan MH. Bacteria and inflammatory cells in fetal membranes do not always cause preterm labor. Pediatr Res. 2005; 57:404–411. [PubMed: 15659699]
7. Yoon BH, Romero R, Moon JB, Shim S-S, Kim M, Kim G, Jun JK. Clinical significance of intra-amniotic inflammation in patients with preterm labor and intact membranes. Am J Obstet Gynecol. 2001; 185:1130–1136. [PubMed: 11717646]
8. Gotsch F, Romero R, Kusanovic JP, Mazaki-Tovi S, Pineles BL, Erez O, Espinoza J, Hassan SS. The fetal inflammatory response syndrome. Clinical obstetrics and gynecology. 2007; 50:652–683. [PubMed: 17762416]
9. Andrews WW, Goldenberg RL, Faye-Petersen O, Cliver S, Goepfert AR, Hauth JC. The Alabama Preterm Birth study: polymorphonuclear and mononuclear cell placental infiltrations, other markers of inflammation, and outcomes in 23- to 32-week preterm newborn infants. Am J Obstet Gynecol. 2006; 195:803–808. [PubMed: 16949415]
10. Weitkamp JH, Guthrie SO, Wong HR, Moldawer LL, Baker HV, Wynn JL. Histological chorioamnionitis shapes the neonatal transcriptomic immune response. Early Hum Dev. 2016; 98:1–6. [PubMed: 27318328]
11. Gomez R, Romero R, Ghezzi F, Yoon BH, Mazor M, Berry SM. The fetal inflammatory response syndrome. Am J Obstet Gynecol. 1998; 179:194–202. [PubMed: 9704787]
12. Chen ML, Allred EN, Hecht JL, Onderdonk A, VanderVeen D, Wallace DK, Leviton A, Dammann O. ELGAN Study. Placenta microbiology and histology and the risk for severe retinopathy of prematurity. Invest Ophthalmol Vis Sci. 2011; 52:7052–7058. [PubMed: 21775664]
13. Wu YW, Colford JM. Chorioamnionitis as a risk factor for cerebral palsy: A meta-analysis. JAMA. 2000; 284:1417–1424. [PubMed: 10989405]
14. Romero R, Espinoza J, Goncalves LF, Gomez R, Medina L, Silva M, Chaiworapongsa T, Yoon BH, Ghezzi F, Lee W. Fetal cardiac dysfunction in preterm premature rupture of membranes. The Journal of Maternal-Fetal & Neonatal Medicine. 2004; 16:146–157. [PubMed: 15590440]
15. Kramer BW, Kallapur S, Newnham J, Jobe AH. Prenatal inflammation and lung development. Seminar Fetal Neonatal Med. 2009; 14:2–7.e1.
16. Leviton A, Hecht JL, Allred EN, Yamamoto H, Fichorova RN, Dammann O. ELGAN Study Investigators. Persistence after birth of systemic inflammation associated with umbilical cord inflammation. J Reprod Immunol. 2011; 90:235–243. [PubMed: 21722967]
17. O'Shea TM, Allred EN, Kuban KC, Dammann O, Paneth N, Fichorova R, Hirtz D, Leviton A. Extremely Low Gestational Age Newborn (ELGAN) Study Investigators. Elevated concentrations of inflammation-related proteins in postnatal blood predict severe developmental delay at 2 years of age in extremely preterm infants. J Pediatr. 2012; 160:395–401.e4. [PubMed: 22000304]
18. Bastek JA, Weber AL, McShea MA, Ryan ME, Elovitz MA. Prenatal inflammation is associated with adverse neonatal outcomes. Am J Obstet Gynecol. 2014; 210:450.e1–450.10. [PubMed: 24361788]

19. Savasan ZA, Chaiworapongsa T, Romero R, Hussein Y, Kusanovic JP, Xu Y, Dong Z, Kim CJ, Hassan SS. Interleukin-19 in fetal systemic inflammation. J Matern Fetal Neonatal Med. 2012; 25:995–1005. [PubMed: 21767236]

20. Kallapur SG, Presicce P, Rueda CM, Jobe AH, Chougnet CA. Fetal immune response to chorioamnionitis. Semin Reprod Med. 2014; 32:56–67. [PubMed: 24390922]

21. Vlassaks E, Gavilanes AW, Bieghs V, Reinartz A, Gassler N, Van Gorp PJ, Gijbels MJ, Bekers O, Zimmermann LJ, Pillow JJ, Polglase GR, Nitsos I, Newnham JP, Kallapur SG, Jobe AH, Shiri-Sverdlov R, Kramer BW. Antenatal exposure to chorioamnionitis affects lipid metabolism in 7-week-old sheep. J Dev Orig Health Dis. 2012; 3:103–110. [PubMed: 25101920]

22. Matsuoka T, Matsubara T, Katayama K, Takeda K, Koga M, Furukawa S. Increase of cord blood cytokine-producing T cells in intrauterine infection. Pediatr Int. 2001; 43:453–457. [PubMed: 11737704]

23. Michalek RD, Gerriets VA, Jacobs SR, Macintyre AN, MacIver NJ, Mason EF, Sullivan SA, Nichols AG, Rathmell JC. Cutting edge: distinct glycolytic and lipid oxidative metabolic programs are essential for effector and regulatory CD4+ T cell subsets. J Immunol. 2011; 186:3299–3303. [PubMed: 21317389]

24. Fernandez-Sesma A, Marukian S, Ebersole BJ, Kaminski D, Park MS, Yuen T, Sealfon SC, García-Sastre A, Moran TM. Influenza virus evades innate and adaptive immunity via the NS1 protein. J Virol. 2006; 80:6295–6304. [PubMed: 16775317]

25. Espinosa E, Ormsby CE, Reyes-Teran G, Asaad R, Sieg SF, Lederman MM. Dissociation of CD154 and cytokine expression patterns in $CD38^{+}$ $CD4^{+}$ memory T cells in chronic HIV-1 infection. J Acquir Immune Defic Syndr. 2010; 55:439–445. [PubMed: 20926955]

26. Kruisbeek AM, Shevach E, Thornton AM. Proliferative assays for T cell function. Current Protocols in Immunology. 2004:3–12.

27. Brown JA, Sherrod SD, Goodwin CR, Brewer B, Yang L, Garbett KA, Li D, McLean JA, Wikswo JP, Mirnics K. Metabolic consequences of interleukin-6 challenge in developing neurons and astroglia. J Neuroinflammation. 2014; 11:183. [PubMed: 25374324]

28. Kessner D, Chambers M, Burke R, Agus D, Mallick P. ProteoWizard: open source software for rapid proteomics tools development. Bioinformatics. 2008; 24:2534–2536. [PubMed: 18606607]

29. Wishart DS. Current progress in computational metabolomics. Briefings in Bioinformatics. 2007; 8:279–293. [PubMed: 17626065]

30. Smith CA, O'Maille G, Want EJ, Qin C, Trauger SA, Brandon TR, Custodio DE, Abagyan R, Siuzdak G. METLIN: a metabolite mass spectral database. Ther Drug Monit. 2005; 27:747–751. [PubMed: 16404815]

31. Sud M, Fahy E, Cotter D, Brown A, Dennis EA, Glass CK, Merrill AH, Murphy RC, Raetz CR, Russell DW, Subramaniam S. LMSD: LIPID MAPS structure database. Nucleic Acids Res. 2007; 35:D527–D532. [PubMed: 17098933]

32. Avula B, Wang YH, Isaac G, Yuk J, Wrona M, Yu K, Khan IA. Metabolomics Based UHPLC-QToF-MS Approach for the Authentication of Various Botanicals and Dietary Supplements. Planta Medica. 2016; 82:OA13.

33. Korn T, Reddy J, Gao W, Bettelli E, Awasthi A, Petersen TR, Bäckström BT, Sobel RA, Wucherpfennig KW, Strom TB, Oukka M, Kuchroo VK. Myelin-specific regulatory T cells accumulate in the CNS but fail to control autoimmune inflammation. Nat Med. 2007; 13:423–431. [PubMed: 17384649]

34. Zhang X, Mozeleski B, Lemoine S, Dériaud E, Lim A, Zhivaki D, Azria E, Le Ray C, Roguet G, Launay O, Vanet A, Leclerc C, Lo-Man R. CD4 T cells with effector memory phenotype and function develop in the sterile environment of the fetus. Sci Transl Med. 2014; 6:238ra72.

35. Weitkamp JH, Koyama T, Rock MT, Correa H, Goettel JA, Matta P, Oswald-Richter K, Rosen MJ, Engelhardt BG, Moore DJ, Polk DB. Necrotising enterocolitis is characterised by disrupted immune regulation and diminished mucosal regulatory (FOXP3)/effector (CD4, CD8) T cell ratios. Gut. 2013; 62:73–82. [PubMed: 22267598]

36. Guerra C, Morris D, Sipin A, Kung S, Franklin M, Gray D, Tanzil M, Guilford F, Khasawneh FT, Venketaraman V. Glutathione and adaptive immune responses against Mycobacterium tuberculosis

infection in healthy and HIV infected individuals. PLoS One. 2011; 6:e28378. [PubMed: 22164280]

37. Munn DH, Mellor AL. Indoleamine 2,3 dioxygenase and metabolic control of immune responses. Trends Immunol. 2013; 34:137–143. [PubMed: 23103127]
38. Buck MD, OSullivan D, Pearce EL. T cell metabolism drives immunity. The Journal of experimental medicine. 2015; 212:1345–1360. [PubMed: 26261266]
39. Michalek RD, Rathmell JC. The metabolic life and times of a T-cell. Immunological reviews. 2010; 236:190–202. [PubMed: 20636818]
40. Härtel C, Adam N, Strunk T, Temming P, Müller-Steinhardt M, Schultz C. Cytokine responses correlate differentially with age in infancy and early childhood. Clin Exp Immunol. 2005; 142:446–453. [PubMed: 16297156]
41. Maródi L. Innate cellular immune responses in newborns. Clinical Immunology. 2006; 118:137–144. [PubMed: 16377252]
42. Herberth G, Bauer M, Gasch M, Hinz D, Röder S, Olek S, Kohajda T, Rolle-Kampczyk U, von Bergen M, Sack U, Borte M, Lehmann I. Lifestyle and Environmental Factors and Their Influence on Newborns Allergy Risk study group. Maternal and cord blood miR-223 expression associates with prenatal tobacco smoke exposure and low regulatory T-cell numbers. J Allergy Clin Immunol. 2014; 133:543–550. [PubMed: 23978443]
43. Kallapur SG, Presicce P, Senthamaraikannan P, Alvarez M, Tarantal AF, Miller LM, Jobe AH, Chougnet CA. Intra-amniotic IL-1β induces fetal inflammation in rhesus monkeys and alters the regulatory T cell/IL-17 balance. J Immunol. 2013; 191:1102–1109. [PubMed: 23794628]
44. Luciano AA, Yu H, Jackson LW, Wolfe LA, Bernstein HB. Preterm labor and chorioamnionitis are associated with neonatal T cell activation. PLoS One. 2011; 6:e16698. [PubMed: 21347427]
45. Uchida K. 4-Hydroxy-2-nonenal: a product and mediator of oxidative stress. Progress in lipid research. 2003; 42:318–343. [PubMed: 12689622]
46. Esterbauer H, Schaur RJR, Zollner H. Chemistry and biochemistry of 4-hydroxynonenal, malonaldehyde and related aldehydes. Free Radic Biol Med. 1990; 11:81–128.
47. Esterbauer H, Eckl P, Ortner A. Possible mutagens derived from lipids and lipid precursors. Mutat Res. 1990; 238:223–233. [PubMed: 2342513]
48. Awasthi YC, Yang Y, Tiwari NK, Patrick B, Sharma A, Li J, Awasthi S. Regulation of 4-hydroxynonenal-mediated signaling by glutathione S-transferases. Free Radic Biol Med. 2004; 37:607–619. [PubMed: 15288119]
49. Spitz DR, Sullivan SJ, Malcolm RR, Roberts RJ. Glutathione dependent metabolism and detoxification of 4-hydroxy-2-nonenal. Free Radical Biology and Medicine. 1991; 11:415–423. [PubMed: 1797627]
50. Yadav UC, Ramana KV, Awasthi YC, Srivastava SK. Glutathione level regulates HNE-induced genotoxicity in human erythroleukemia cells. Toxicol Appl Pharmacol. 2008; 227:257–264. [PubMed: 18096195]
51. Hamilos DL, Wedner HJ. The role of glutathione in lymphocyte activation. I. Comparison of inhibitory effects of buthionine sulfoximine and 2-cyclohexene-1-one by nuclear size transformation. J Immunol. 1985; 135:2740–2747. [PubMed: 4031498]
52. Fischman CM, Udey MC, Kurtz M, Wedner HJ. Inhibition of lectin-induced lymphocyte activation by 2-cyclohexene-1-one: decreased intracellular glutathione inhibits an early event in the activation sequence. J Immunol. 1981; 127:2257–2262. [PubMed: 6975313]
53. Wedner HJ, Bahn G, Gordon LK, Fischman CM. Inhibition of lectin-induced lymphocyte activation by 2-cyclohexene-1-one: analysis of DNA synthesis in individual cells by BUdR quenching of Hoechst 33258. Int J Immunopharmacol. 1985; 7:25–30. [PubMed: 2581906]
54. Dröge W, Pottmeyer-Gerber C, Schmidt H, Nick S. Glutathione augments the activation of cytotoxic T lymphocytes in vivo. Immunobiology. 1986; 172:151–156. [PubMed: 3490430]
55. Peterson JD, Herzenberg LA, Vasquez K, Waltenbaugh C. Glutathione levels in antigen-presenting cells modulate Th1 versus Th2 response patterns. Proc Natl Acad Sci U S A. 1998; 95:3071–3076. [PubMed: 9501217]

56. Smyth MJ. Glutathione modulates activation-dependent proliferation of human peripheral blood lymphocyte populations without regulating their activated function. J Immunol. 1991; 146:1921–1927. [PubMed: 2005386]
57. Keszthelyi D, Troost FJ, Masclee AA. Understanding the role of tryptophan and serotonin metabolism in gastrointestinal function. Neurogastroenterol Motil. 2009; 21:1239–1249. [PubMed: 19650771]
58. Werner ER, Werner-Felmayer G, Fuchs D, Hausen A, Reibnegger G, Wachter H. Parallel induction of tetrahydrobiopterin biosynthesis and indoleamine 2,3-dioxygenase activity in human cells and cell lines by interferon-gamma. Biochem J. 1989; 262:861–866. [PubMed: 2511835]
59. Yoshida R, Nukiwa T, Watanabe Y, Fujiwara M, Hirata F, Hayaishi O. Regulation of indoleamine 2,3-dioxygenase activity in the small intestine and the epididymis of mice. Arch Biochem Biophys. 1980; 203:343–351. [PubMed: 6967714]
60. Yoshida R, Imanishi J, Oku T, Kishida T, Hayaishi O. Induction of pulmonary indoleamine 2, 3-dioxygenase by interferon. Proceedings of the National Academy of Sciences. 1981; 78:129–132.
61. Grant RS, Naif H, Espinosa M, Kapoor V. IDO induction in IFN-gamma activated astroglia: a role in improving cell viability during oxidative stress. Redox Rep. 2000; 5:101–104. [PubMed: 10939283]
62. Moffett JR, Namboodiri MAA. Tryptophan and the immune response. Immunology and cell biology. 2003; 81:247–265. [PubMed: 12848846]
63. Mosmann TR, Coffman RL. Heterogeneity of cytokine secretion patterns and functions of helper T cells. Adv Immunol. 1989; 46:111–147. [PubMed: 2528896]
64. Mosmann TR, Sad S. The expanding universe of T-cell subsets: Th1, Th2 and more. Immunol Today. 1996; 17:138–146. [PubMed: 8820272]
65. Cook-Mills JM, Cohen RL, Perlman RL, Chambers DA. Inhibition of lymphocyte activation by catecholamines: evidence for a non-classical mechanism of catecholamine action. Immunology. 1995; 85:544–549. [PubMed: 7558147]
66. Bergquist J, Tarkowski A, Ekman R, Ewing A. Discovery of endogenous catecholamines in lymphocytes and evidence for catecholamine regulation of lymphocyte function via an autocrine loop. Proc Natl Acad Sci U S A. 1994; 91:12912–12916. [PubMed: 7809145]
67. Swanson MA, Lee WT, Sanders VM. IFN-γ production by Th1 cells generated from naive CD4+ T cells exposed to norepinephrine. The Journal of Immunology. 2001; 166:232–240. [PubMed: 11123297]
68. Josefsson E, Bergquist J, Ekman R, Tarkowski A. Catecholamines are synthesized by mouse lymphocytes and regulate function of these cells by induction of apoptosis. Immunology. 1996; 88:140–146. [PubMed: 8707341]
69. Alaniz RC, Thomas SA, Perez-Melgosa M, Mueller K, Farr AG, Palmiter RD, Wilson CB. Dopamine beta-hydroxylase deficiency impairs cellular immunity. Proc Natl Acad Sci U S A. 1999; 96:2274–2278. [PubMed: 10051631]
70. Klesney-Tait J, Turnbull IR, Colonna M. The TREM receptor family and signal integration. Nat Immunol. 2006; 7:1266–1273. [PubMed: 17110943]
71. Wahle M, Hanefeld G, Brunn S, Straub RH, Wagner U, Krause A, Häntzschel H, Baerwald CG. Failure of catecholamines to shift T-cell cytokine responses toward a Th2 profile in patients with rheumatoid arthritis. Arthritis Res Ther. 2006; 8:R138. [PubMed: 16889669]
72. Swanson MA, Lee WT, Sanders VM. IFN-γ production by Th1 cells generated from naive CD4+ T cells exposed to norepinephrine. The Journal of Immunology. 2001; 166:232–240. [PubMed: 11123297]
73. Herwald, H., Egesten, A. Sepsis--Pro-Inflammatory and Anti-Inflammatory Responses. Karger Medical and Scientific Publishers; 2011.
74. Mehta D. Lysophosphatidylcholine: an enigmatic lysolipid. American Journal of Physiology-Lung Cellular and Molecular Physiology. 2005; 289:L174–L175. [PubMed: 16002999]
75. Marusic S, Thakker P, Pelker JW, Stedman NL, Lee KL, McKew JC, Han L, Xu X, Wolf SF, Borey AJ, Cui J, Shen MW, Donahue F, Hassan-Zahraee M, Leach MW, Shimizu T, Clark JD. Blockade of cytosolic phospholipase A2 alpha prevents experimental autoimmune encephalomyelitis and

diminishes development of Th1 and Th17 responses. J Neuroimmunol. 2008; 204:29–37. [PubMed: 18829119]

76. Marusic S, Leach MW, Pelker JW, Azoitei ML, Uozumi N, Cui J, Shen MW, DeClercq CM, Miyashiro JS, Carito BA, Thakker P, Simmons DL, Leonard JP, Shimizu T, Clark JD. Cytosolic phospholipase A2 alpha-deficient mice are resistant to experimental autoimmune encephalomyelitis. J Exp Med. 2005; 202:841–851. [PubMed: 16172261]
77. Berger A. Th1 and Th2 responses: what are they? Bmj. 2000; 321:424. [PubMed: 10938051]
78. Melville JM, Moss TJ. The immune consequences of preterm birth. Front Neurosci. 2013; 7:79. [PubMed: 23734091]

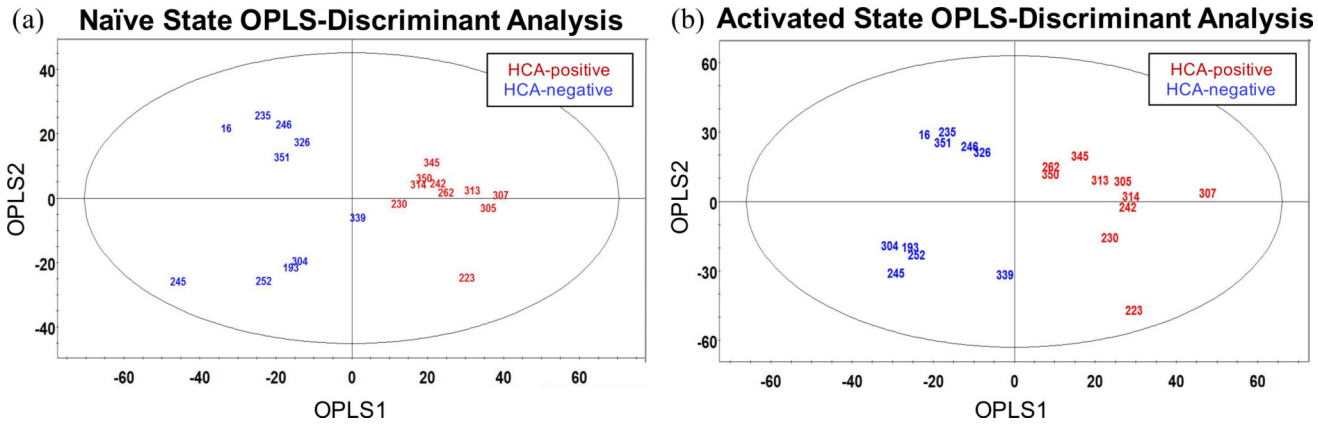

Figure 1. Preterm CD4$^+$ T lymphocytes exposed to HCA exhibit distinct exo-metabolomic profiles in both naïve and activated states

(a) *left* OPLS-DA score plot illustrates the distinct exo-metabolomic signatures of naive HCA-positive and -negative CD4$^+$ T lymphocytes. Mass spectral data were normalized and Pareto scaled before analysis. OPLS1 resolves the two sample types, explaining 27.8% of the covariance in the data. OPLS2 explains 21.9% of the variance between spectra. The ellipse denotes the 95% significance limit of the model, as defined by Hotelling's *t*-test. This experiment was independently performed once; each UPLC-IM-MS measurement was performed in triplicate (technical replicates).

(b) *right* OPLS-DA score plot illustrates the distinct exo-metabolomic signatures of activated HCA-positive and -negative CD4$^+$ T lymphocytes. Mass spectral data were normalized and Pareto scaled before analysis. OPLS1 resolves the two sample types, explaining 23.3% of the covariance between spectra. OPLS2 explains 28.6% of the variance between spectra. The ellipse denotes the 95% significance limit of the model, as defined by Hotelling's *t*-test. This experiment was independently performed once; each UPLC-IM-MS measurement was performed in triplicate (technical replicates).

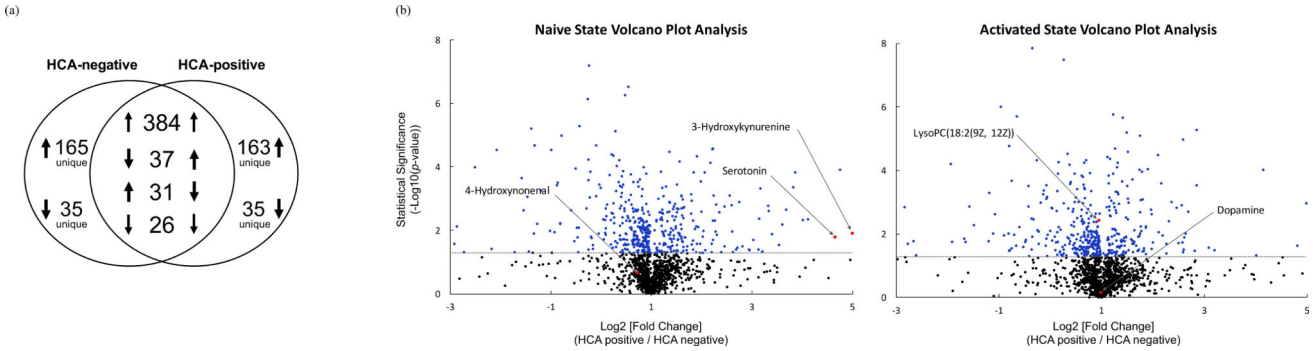

Figure 2. Exposure to HCA alters CD4$^+$ T lymphocyte exo-metabolome production and consumption patterns following SEB/CD28-induced activation

(a) Venn diagram illustrating the production and consumption of differentially expressed metabolites (|FC| > 1, $p < 0.05$) upon stimulation with SEB/CD28. Numerals denote the number of differentially expressed metabolites and arrows denote the directionality of change following stimulation.

(b) Volcano plot analyses of HCA-positive and –negative CD4$^+$ T lymphocyte exo-metabolome in the naïve and activated states. Comparisons of all metabolites from samples exposed to *in utero* HCA ($n = 10$) and not exposed to HCA ($n = 10$). Volcano plots display the relationship between the log2 [FC] and its statistical significance using a scatter plot view. The y-axis represents the negative log10 of *p*-values (a higher value indicates greater statistical significance) and the x-axis signifies the log2 [FC] (normalized abundance were used to compute these values). Black points indicate metabolites expressed at insignificantly different levels in both sample types ($p > 0.05$). Blue points indicate metabolites expressed at significantly different levels in one sample type over the other ($p < 0.05$). *Putatively identified metabolites are shown in red and labeled.*

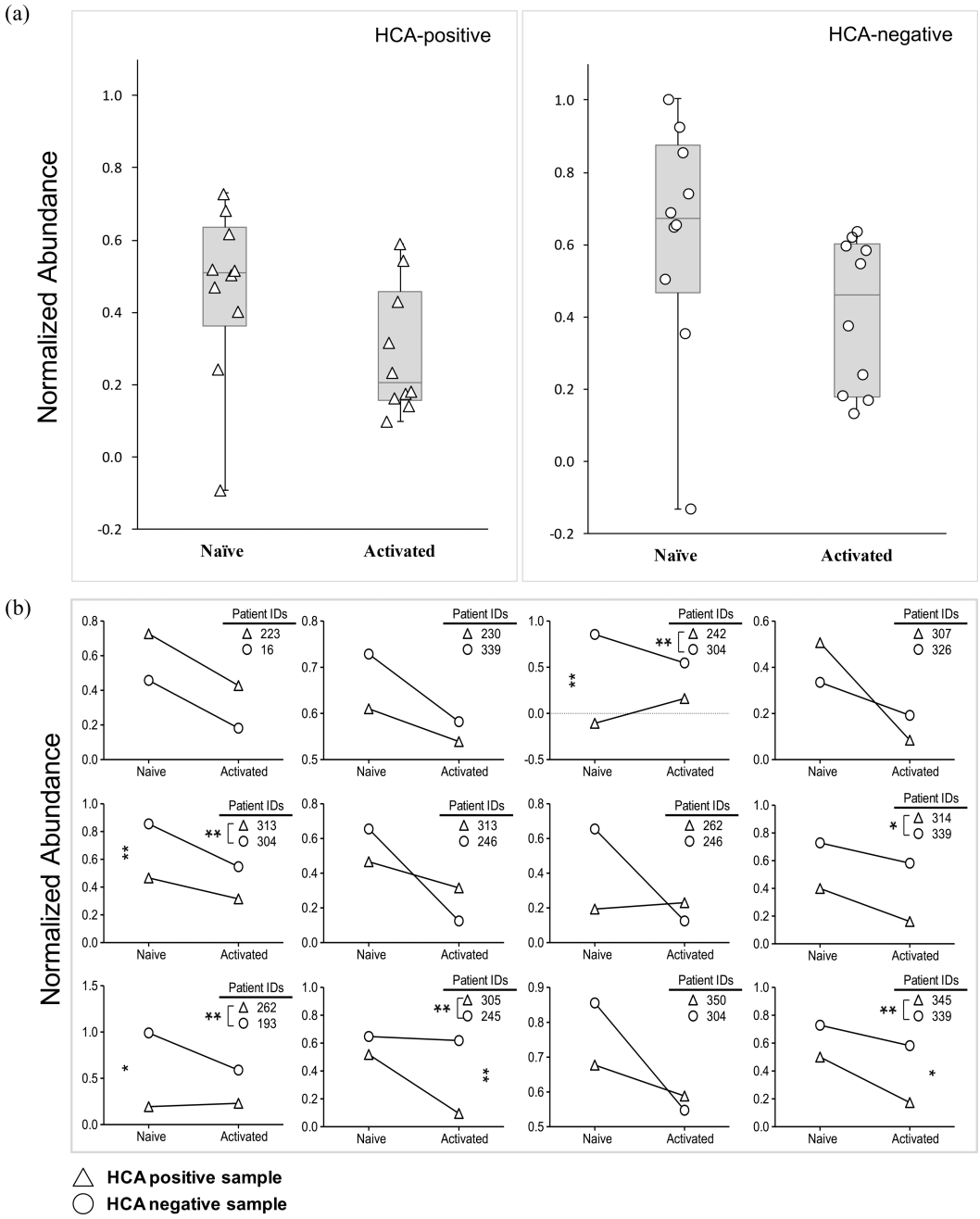

Figure 3. Naïve CD4$^+$ T lymphocytes exposed to HCA exhibited decreased abundances of 4-HNE

(a) Box and whisker-plot analysis with scatter overlay depicting the normalized abundance values of the putatively identified metabolite, 4-HNE (*m/z* = 195.07, RT = 1.03 min). Error bars signify maximum and minimum detected values. HCA-positive samples are denoted by triangles and HCA-negative samples by circles. Median values are also shown.

(b) Pairwise comparison of the normalized abundance of 4-HNE (*m/z* = 195.07, RT = 1.03 min) in the naïve and activated states. Each graph depicts the results of 2-way repeated measures ANOVA. HCA-positive samples are represented with triangles while HCA-

negative samples are represented by circles. Statistical significance is denoted with stars ($p < 0.05$ = *; $p < 0.01$ = **).

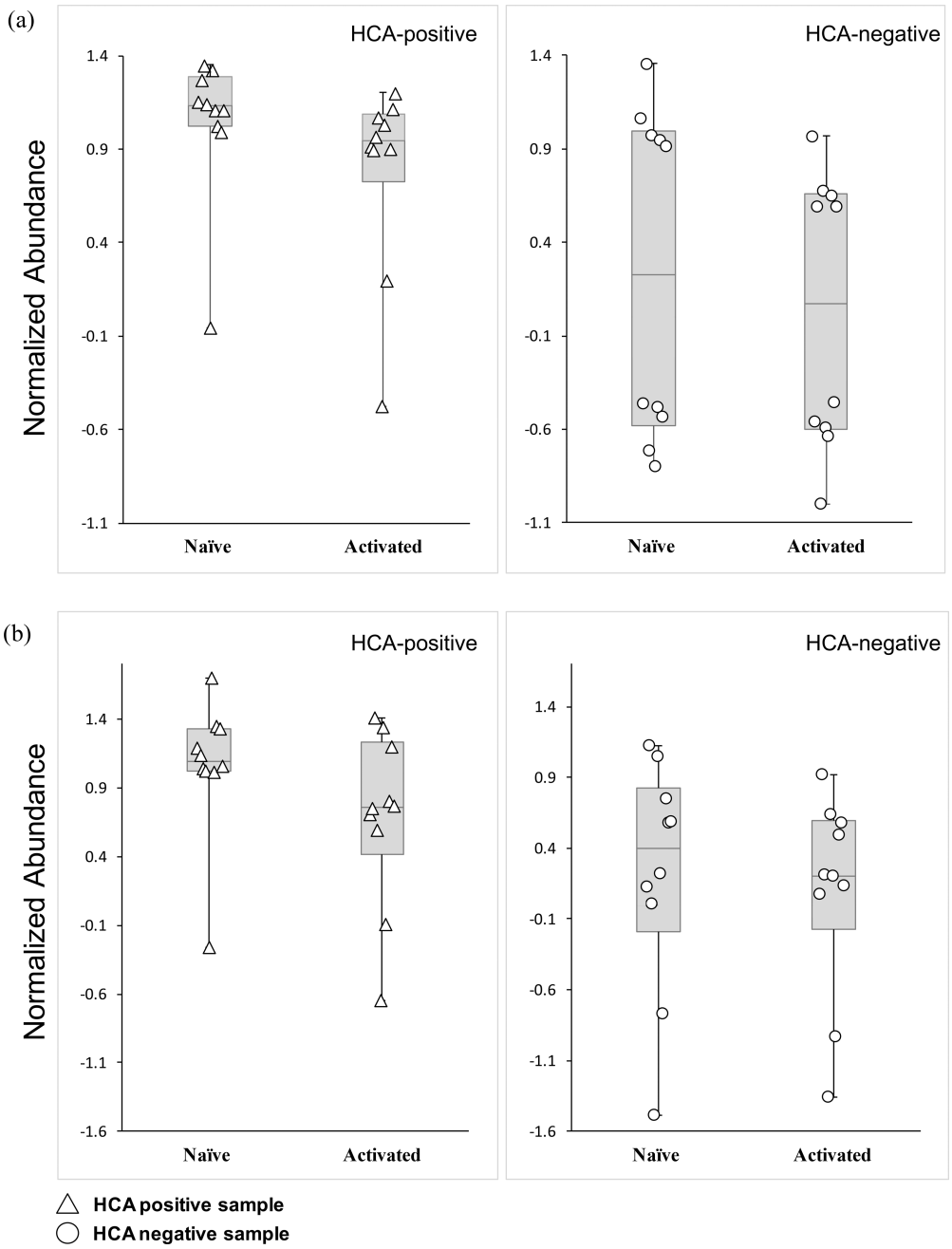

Figure 4. Exposure to HCA alters tryptophan metabolism in naïve and activated CD4$^+$ T lymphocytes

(a) Box and whisker-plot analysis with scatter overlay depicting the normalized abundance values of the putatively identified metabolite, 5-HT (*m/z* 177.08, RT 2.57 min). Error bars signify maximum and minimum detected values. HCA-positive samples are denoted by triangles and HCA-negative samples by circles. Median values are also shown.

(b) Box and whisker-plot analysis with scatter overlay depicting the normalized abundance values of the putatively identified metabolite, 3-HK (*m/z* 225.09, RT 1.25 min). Error bars signify maximum and minimum detected values. HCA-positive samples are denoted by triangles and HCA-negative samples by circles. Median values are also shown.

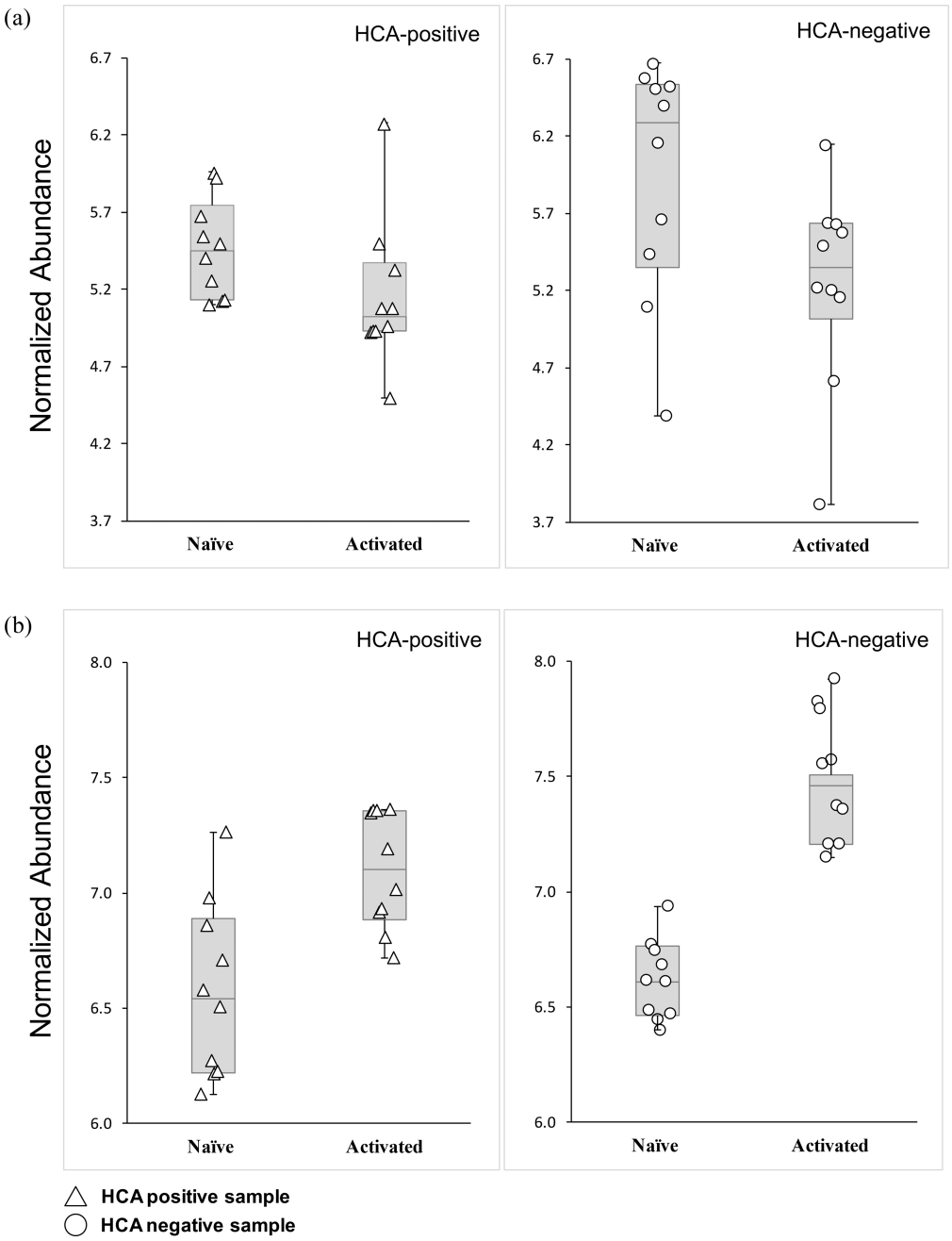

Figure 5. Exposure to HCA does not affect DA and LPC metabolism in naïve and activated CD4$^+$ T lymphocytes

(a) Box and whisker-plot analyses with scatter overlay depicting the normalized abundance values of the putatively identified metabolite, DA (*m/z* 176.07, RT 4.63 min). Error bars signify maximum and minimum detected values. HCA-positive samples are denoted by triangles and HCA-negative samples by circles. Median values are also shown.

(c) Box and whisker-plot analysis with scatter overlay depicting the normalized abundance values of the putatively identified metabolite, LPC (18:2(9Z, 12Z)) (*m/z* 520.35, RT 10.49 min). Error bars signify maximum and minimum detected values. HCA-positive samples are denoted by triangles and HCA-negative samples by circles. Median values are also shown.

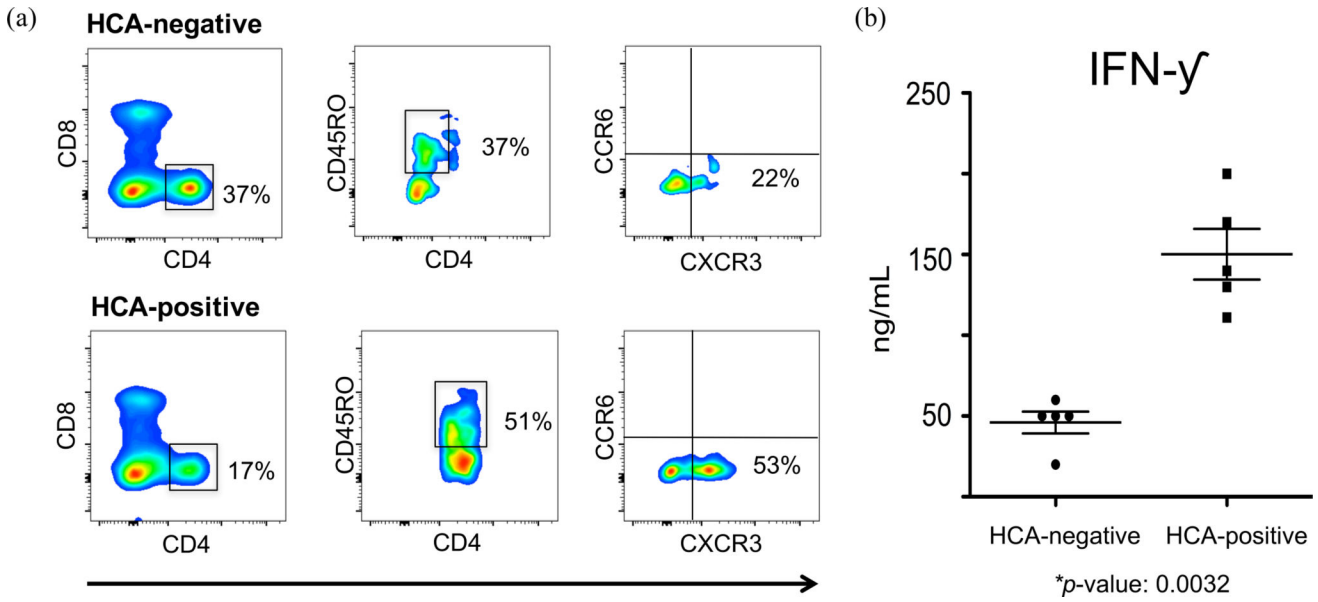

Figure 6. Exposure to HCA increases the percentage of memory CD4$^+$ T lymphocytes exhibiting a T_H1 phenotype and IFN-γ secretion

(a) Representative analytic flow cytometry plot of CD4$^+$ T lymphocytes collected on postnatal day 10 from 5 pairs of preterm infants matched for gestational age, day of blood draw, sex, race, prenatal steroid exposure, and delivery mode. Each pair consisted of one HCA-positive and one HCA-negative patient (10 samples total). Here we are showing data from two 24 weeks gestation female Hispanic infants, delivered via Cesarean section following prenatal steroid prophylaxis. One infant was exposed to *in utero* HCA while the other showed no clinical or histological signs of chorioamnionitis.

(b) IFN-γ secretions were measured by Luminex technology. Cells were collected from 5 pairs of preterm infants matched for gestational age, day of blood draw, sex, race, prenatal steroid exposure, and delivery mode. Each pair consisted of one HCA-positive and one HCA-negative patient (10 samples total). Paired t-test was used to determine statistical significant differences. This experiment was independently performed once, without replicates.

J Immunol. Author manuscript; available in PMC 2018 November 01.

Table I

Characteristics of patient samples[1]

HCA-negative samples (n = 10)

Patient ID	Gestational Age (wks., days)	Sex	Race	Delivery Mode	Day of Blood Draw (after birth)	Exposure to Pre-Natal Antibiotics	Exposure to Post-Natal Antibiotics	Clinical Signs of Funisitis in Fetus
339	26, 5	M	African American	Cesarean	10	Y	Amp/Gen through DOL 3	N/A
351	25, 5	M	Caucasian	Cesarean	5	Y	Amp/Gen through DOL 7	N/A
326	27, 5	M	Caucasian	Cesarean	10	Y	Amp/Gen through DOL 2	N/A
245	26, 5	M	Caucasian	Cesarean	10	Y	Amp/Gen through DOL 2	N/A
246	26, 5	F	Caucasian	Vaginal	10	N	Amp/Gen through DOL 7	N/A
16	26, 5	F	African American	Vaginal	5	Y	Amp/Gen through DOL 2	N/A
235	27, 5	F	Caucasian	Cesarean	5	Y	Amp/Gen through DOL 2	N/A
193	27, 5	F	Caucasian	Cesarean	10	Y	Amp/Gen through DOL 2	N/A
304	25, 6	F	Caucasian	Cesarean	10	Y	Amp/Gen through DOL 6 & Van on DOL 3 only	N/A
252	26, 6	M	Caucasian	Cesarean	5	N	Amp/Gen through DOL 3 & Gen DOL 10 only	N/A

HCA-positive samples (n = 10)

Patient ID	Gestational Age (wks., days)	Sex	Race	Delivery Mode	Day of Blood Draw (after birth)	Exposure to Pre-Natal Antibiotics	Exposure to Post-Natal Antibiotics	Clinical Signs of Funisitis in Fetus
345	27, 5	M	African American	Cesarean	10	Y	Amp/Gen through DOL 6	Stage II FIRS
230	26, 4	M	African American	Vaginal	10	Y	Amp/Gen through DOL 2	None
314	27, 6	M	African American	Vaginal	10	Y	Amp/Gen through DOL 7	Stage II FIRS
305	26, 6	M	Caucasian	Cesarean	10	Y	Amp/Gen through DOL 6	None
262	28, 5	F	Caucasian	Vaginal	10	Y	Amp/Gen through DOL 9	Stage II FIRS
242	25, 4	F	Caucasian	Cesarean	10	Y	Amp/Gen through DOL 7	Stage II FIRS
350	24, 6	F	Caucasian	Cesarean	10	Y	Amp through DOL 10 & Gen DOL 6	Stage II FIRS
223	27, 5	F	African American	Vaginal	10	Y	Amp through DOL 10, Gen DOL 3 & Cfp DOL 3–10 only	Stage II FIRS
307	28, 6	M	Caucasian	Cesarean	10	Y	Amp/Gen through DOL 6 & Ctx DOL 2	Stage I FIRS

313	25, 5	F	Caucasian	Vaginal	10	Y	Amp/Gen through DOL 2 & Gen/Van DOL 9, 10 only	Stage II FIRS

Statistical Analyses

	Gestational Age	Sex	Race	Delivery Mode	Day of Blood Draw	Exposure to Pre-Natal Antibiotics	Exposure to Post-Natal Antibiotics
p-value	0.69	1	0.36	0.18	*0.04	0.15	*0.03

[1]Antibiotic abbreviations are as follows: Amp, Ampicillin; Gen, Gentamicin; Van, Vancomycin; Cfp, Cefepime; Ctx, Ceftotaxime.

Table II

List of putatively identified metabolites and their mass accuracy.

Feature	Experimental mass-to-charge ratio pairs (*m/z*)	Retention Time (min)	Putative Molecular Identification	Mass Accuracy (ppm)
1	195.07	1.03	4-Hydroxynonenal (4-HNE)	12.80
2	177.08	2.57	Serotonin (5-HT)	17.00
3	225.09	1.25	3-Hydroxykynurenine (3-HK)	20.25
4	176.07	4.63	Dopamine (DA)	13.10
5	520.35	10.49	LysoPC(18:2(9Z, 12Z)) (LPC)	28.04